198. Forward Electron Scattering in Benzene; Forbidden Transitions and Excitation Functions

by **Michael Allan**

Institut de chimie physique de l'Université, CH-1700 Fribourg

(6.VIII.82)

Summary

A systematic study of vibronic excitation in benzene *via* forward electron scattering was carried out using a novel type of a trochoidal electron spectrometer. Energy-loss spectra in the energy range 1.0–9.5 eV, with residual energies 0.03–20 eV as well as excitation functions for individual vibrational levels of some of the triplet and singlet states are presented and discussed. Following observations were made. 1) A new s-type *Rydberg* series with quantum defect $\delta = 0.86$. 2) Additional information on the complex 6–6.5 eV band. 3) A new core excited shape resonance at 6.5 eV. 4) A narrow *Feshbach* resonance at 5.87 eV. The new spectrometer is suggested as a tool for routine study of forbidden transitions and negative ion states in organic molecules.

1. Introduction. – Benzene is a prototype example of an aromatic system and, therefore, its electronic structure has been of great interest to both theorists and experimentalists. This fact is reflected in the large amount of publications on this subject. The studies on the valence transitions up to 1978 has been summarized in a review article by *Kupperman et al.* [1]. Combined results of a number of experimental methods and theory helped to identify a number of transitions but some questions still remain unanswered. The low-energy region up to 5.8 eV appears to be well-understood. Three triplet and one singlet states, $T_1{}^3B_{1u}$, $T_2{}^3E_{1u}$, $S_1{}^1B_{2u}$, and $T_3{}^3B_{2u}$, resulting from the $e_{1g} - e_{2u}$ $\pi - \pi^*$-promotion were identified in this region. The remaining two $e_{1g} - e_{2u}$ singlets states, $S_2{}^1B_{1u}$ and $S_3{}^1E_{1u}$, have been identified at 6.0 and 6.9 eV. Beyond that the electronic structure at higher energies, 5.9–7.5 eV is much less certain. Particularly in the 6–6.5 eV region with a number of overlapping bands, each subsequent investigation revealed new details [2] [3] [4], but these still cannot be considered as fully understood. In the *Rydberg* region, optical absorption work revealed four series, one of p symmetry ($\sigma = 0.44$) and three of f-symmetry ($\sigma = 0.08$, 0.06, and 0.01). The situation is discussed in the recent publication of *Bolovinos et al.* [5]. The more recent electron impact study of *Wilden & Comer* [4] brought further insight. A fourth triplet state, $^3E_{2g}$, was identified at 6.11 eV. A sharp peak was observed at 6.32 eV and tentatively assigned

0018-019X/82/7/2008-16$01.00/0

to an electric-quadrupole-allowed $^1E_{2g}$-transition, and finally an electric dipole-forbidden d-type *Rydberg* series ($\delta = 0.266$) was observed.

Noteworthy is the major contribution to the present understanding of the benzene electronic structure achieved by electron impact spectroscopy. It is mainly due to its capability to detect dipole-forbidden transitions, mostly singlet-triplet, not visible in optical absorption spectra, and to identify them as such by their incident electron energy and angular dependencies. Electron-scattering experiments have also supplied information about negative ion states or resonances of benzene. General properties of such states are described by *Schulz* [6]. Electron transmission spectroscopy has identified two shape resonances, $^2E_{2u}$ and $^2B_{2g}$ which result from electron capture in the unoccupied e_{2u} and b_{2g} orbitals in benzene. The details are summarized by *Jordan & Burrow* [7]. Luminiscence and total metastable excitation by electron impact measured by *Smyth et al.* [8] as well as vibrational and first-triplet excitation measured by *Azria & Schulz* [9] have given information about higher excited states of benzene anion. The results were summarized by the latter authors, and totally seven features were identified and labeled a–g. Despite these achievements the electron scattering experiments have not become widely used for study of chemically interesting systems. This is mainly because of the complexity and high cost of the electrostatical instruments commonly used and the difficult experimental 'art' of handling slow electrons.

In this paper a systematic study of electronic excitation in benzene using a new, simpler trochoidal electron spectrometer is presented. This type of instrument is intrinsically less versatile than the conventional electrostatic spectrometer, because it does not allow angle variation of scattered electrons, but it offers certain other practical advantages. The results are compared with previous experiments and several new findings are presented. The suitability of the new instrument for routine study of compounds of chemical interest is discussed.

2. Experimental. – Details of the new trochoidal electron spectrometer will be reported later and only a brief description is given here. The use of trochoidal motion of electrons in crossed electric and magnetic fields for energy dispersion has been first reported by *Stamatovic & Schulz* [10]. The trochoidal monochromator has been used extensively to prepare monoenergetic electron beams for electron

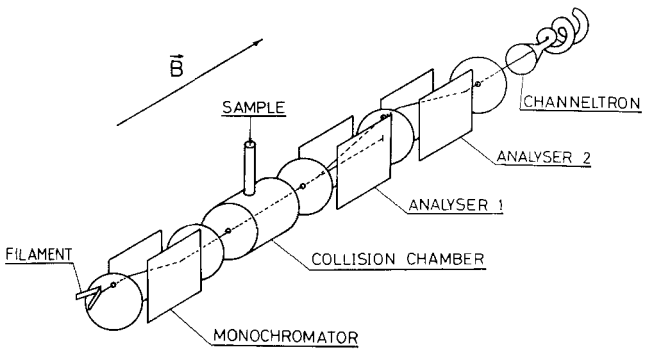

Fig. 1. *Schematic diagram of the apparatus*

transmission [6] [7], and dissociative attachment studies [6]. Its use for scattered-electron energy analysis has been attempted only a few times [11] [12] and a performance which would allow routine use has not been achieved.

The present instrument *(Fig. 1)* uses trochoidal monochromators both to prepare a beam of monoenergetic electrons and to analyze the energies of forward-scattered electrons (the former will be subsequently called monochromator and the latter analyzer). In the present instrument the concept has been further developed as to allow routine study of complex molecules; that is, a low background level and a routine resolution of 0.03–0.04 eV were realized. The most important feature is the use of two analyzers in series. The main effect of the double analyzer is a large attenuation of the unscattered electron beam which enters the analyzer directly at the zero-degrees geometry and tends to cause a large background.

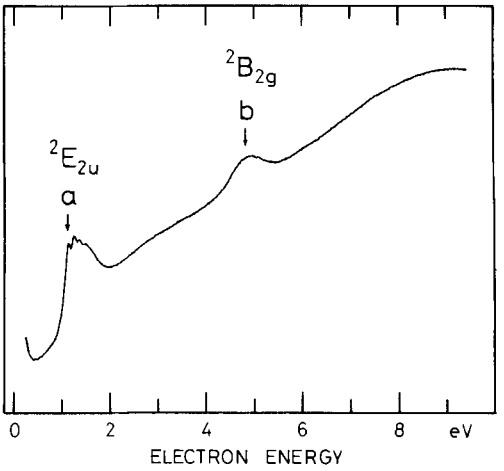

Fig. 2. *Electron transmission spectrum in benzene* (The curve shows the 'total' cross section Q_t (in arbitrary units) obtained from the incident and transmitted currents I_0 and I_t according to the formula $I_t = I_0 \exp(-NQ_tL)$ [6], where N is the gas density and L length of the collision chamber. Zero is offset. The curve is not identical to the correct total cross section as explained in the text)

The instrument can perform three distinct experiments: electron transmission, electron energy loss and excitation-function measurements. In the first experiment all parts of the analyzer are shorted together and used to collect the total current emerging from the collision chamber. The well-known [7] transmission spectrum of benzene is given in *Figure 2* as an illustration. The curve is related to the total scattering cross section but it is not the correct total cross section due to the incomplete rejection of scattered electrons in this type of experiment. A detailed discussion of the phenomenon has been given recently by *Johnston & Burrow* [13]. Usually the derivative of the transmitted current is reported but this capability is not yet incorporated in the experiment. In the energy loss experiment the analyzer is set to detect electrons of a given fixed energy and the incident electron energy is varied by means of a variable potential applied to the monochromator. Excitation pro-

cesses at a fixed energy above threshold are thus recorded. The sensitivity of the instrument across the energy loss spectrum is constant. The excitation function is recorded by setting the instrument for a fixed energy-loss and varying both the monochromator and analyzer energies synchronously to obtain the cross section for excitation a given energy-loss feature as a function of incident energy. The transmission of the analyzer increases rapidly with decreasing scattered electron energy and the raw excitation spectrum must be corrected for this variation. The uniform He-ionization continuum near threshold predicted by *Wannier* [14] and experimentally verified by *Cvejanović & Read* [15] and *Spence* [16], has been used for calibration of the analyzer transmission function as described by *Pichou et al.* [17]. *Figure 3* shows the curves obtained with the present instrument. First-order prediction of the trochoidal analyzer transmission function is based on the assumption

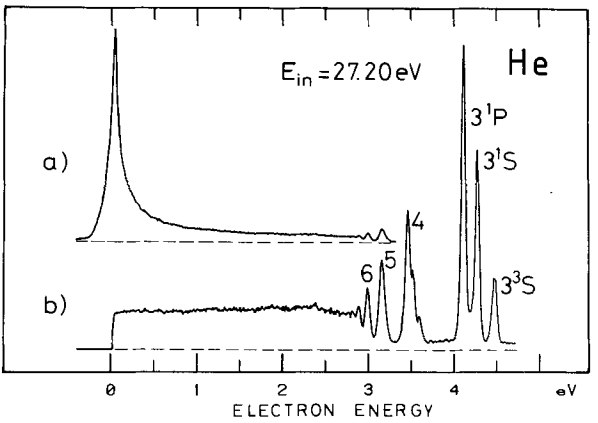

Fig. 3. *Energy-loss spectrum of the ionization continuum in He, recorded with constant incident energy, which was used for calibration of the analyzer transmission* (Curve a is the raw data, curve b is corrected for analyzer transmission function)

that only electrons spiralling with *Larmor* radii smaller than a certain constant value, given in the first approximation by the size of the analyzer entrance aperture, can enter the analyzer. Thus only electrons with a perpendicular velocity less then a certain fixed value given by the aperture size and the magnetic field strength will be detected. This results in an analyzer acceptance angle inversely proportional to total electron velocity or analyzer transmission inversely proportional to the electron energy. When the raw data, curve a in *Figure 3* is corrected for this variation, that is, multiplied by energy, an essentially flat function is obtained. The only imperfection is a slow and linear rise with energy due to second-order effects not included in the above consideration. Therefore a small, linear, second-order empirical correction was applied to the data. The result, curve b in *Figure 3*, is a function constant within $\pm 20\%$ from 0.05 to 2.5 eV. This correction procedure was applied to all excitation functions in this paper. The variation of acceptance angle with residual energy must be kept in mind while interpreting the spectra. While at large residual energies the instrument is a truly zero-degrees spectrometer, at low energies cross

sections averaged over a large acceptance angle are obtained[1]). In the extreme of treshold excitation (residual energy 0.03 eV) the acceptance half angle can approach 90°. This feature must be considered undesirable when a precise knowledge of the scattering angle is required. On the other hand this feature could improve the instrument's capacity to detect forbidden transitions near threshold and is thus desirable from the practical point of view of a chemist who is interested in the electronic structure of a molecule and less in the exact details of the scattering process.

The electron energy loss scale was calibrated on sharp features in pure vibrational as well as vibronic excitation in N_2. It is accurate to 0.02 eV. The incident electron energy was calibrated on the 0.07 eV peak of electrons detached from N^- [18], the first maximum in N_2 $v=1$ excitation function at 1.97 eV [15] and on the 19.37 eV resonance in He. It is accurate to ± 0.04 eV. Sample pressure for transmission experiments is chosen to obtain a reasonable attenuation of the electron beam (30–50%). In N_2 this corresponds to about 10^{-2} mbar, as estimated from the beam attenuation and the known total cross section. Sample pressure used in energy loss measurements were at least a factor of 5 lower. Instrument background pressure during measurement was less than 5×10^{-7} mbar (uncorrected *Penning* gauge reading). Spectroscopic-grade benzene was used without further purification except for degassing.

3. Results and discussion. – The global energy-loss spectrum is presented in *Figure 4*. The spectrum is divided into regions numbered 0–5 and will be discussed individually below. The broad peak in region 0 is due to pure vibrational transitions. Excitation of high vibrational levels in this energy range is selectively enhanced by the first, short-lived negative ion state at 1.15 eV, well-known from electron transmission experiments [7]. The density of vibrational states at 1–2 eV excitation energy is high, the individual levels are no longer resolved and they appear as a quasicontinuum. The broad hump-shifts to the left in the energy-loss spectrum with increasing residual energies. The selective enhancement of pure vibrational excitation occurs at the energy of the resonance, that is at a given incident energy. This property distinguishes it from features associated with a particular electronic transition which remain fixed at the energy-loss scale with increasing residual energy. The pure vibrational excitation will not be further discussed in this paper. The bands in the regions 1–5 are mostly due to excitation of valence states. The structure in the 7.5–9.2 eV region is predominantly *Rydberg*-state excitation. It is superimposed on a quasicontinuum caused probably by high-valence transitions, possibly including such involving σ-orbitals. Above 9.25 eV an additional continuum due to ionization appears. This paper is concerned with valence and *Rydberg* transitions in the 3.5–9.25 eV range as well as the negative ion states involved in their excitation.

---

[1]) Upper limit on the perpendicular electron velocity accepted by the analyzer is obtained from instrument resolution. Assuming 30 meV band-width of the analyzer part alone results in an upper limit on acceptance half angle of 20° at 0.25 eV, 10° at 1.0 eV, and 4.5° at 5 eV. The true acceptance angle is smaller because of the finite contribution of analyzer axial band-width to the overall resolution.

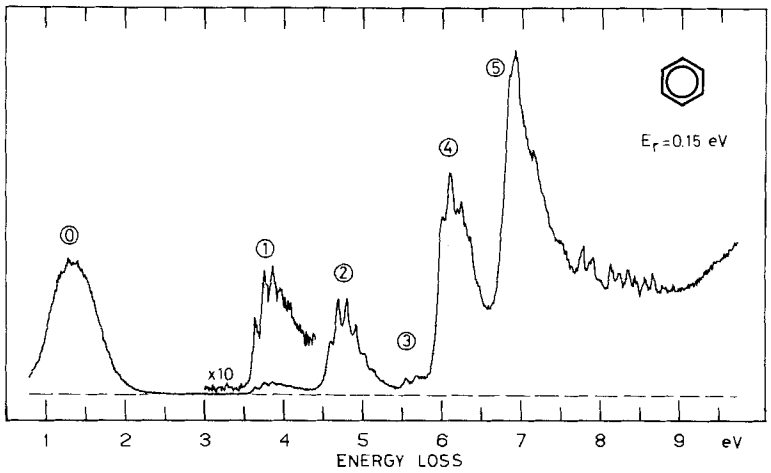

Fig. 4. *Global energy-loss spectrum* (Region 0 is pure vibrational excitation, regions 1–5 are predominantly valence, at this residual energy mostly singlet-triplet transitions. *Rydberg* transitions cause the structure above region 5)

3.1. Valence transitions. The relative intensity of the individual transitions is a function of residual energy, as illustrated in *Figure 5*[2]). At low residual energies the spectrum is dominated by the three lowest triplet transitions in the regions 1, 2 and 3. The present low-energy (0–2 eV) forward-scattering spectra are very similar to the spectra obtained previously with intermediate (10 eV) residual energies and large scattering angles in both gaseous [4] and solid [19] phases. At 20 eV the relative intensity of the triplet states has dropped drastically and the spectrum is nearly identical to an optical absorption spectrum such as given in [5] both in relative intensities of the electronic transitions and the envelopes of the individual bands. At intermediate energies the singlet and triplet bands overlap. Region 4 appears to be far more complex and deserves special attention. At high residual energy it is dominated by the dipole allowed $S_2{}^1B_{1u}$ state. In early work *Lassettre et al.* [2] observed intensity variation across this band with changing residual energy and scattering angle and suggested that a second transition overlaps with the dipole-allowed one. The observation was later confirmed by *Doering* [3]. *Wilden & Comer* [4] investigated this region with better resolution at a number of scattering angles and a residual energy of 10 eV. They discovered a new progression at a large angle (60°) and assigned it to the $^3E_{2g}$ state expected in this energy region. At intermediate angles (10–40°) they clearly discerned a sharp peak at 6.32 eV, responsible for the intensity variation in the earlier work. Its angular dependence is consistent with an electric quadrupole transition. *Wilden & Comer* consider its assignment to either the $^1E_{2g}$ valence state or a *Rydberg* state of the same symmetry. The former assignment was preferred because higher members of a corresponding *Rydberg* series were not present in their spectra. The results obtained with the present

[2]) The spectra have been plotted to the same vertical height for convenience in this and all following figures *(Fig. 6–13)* in this paper.

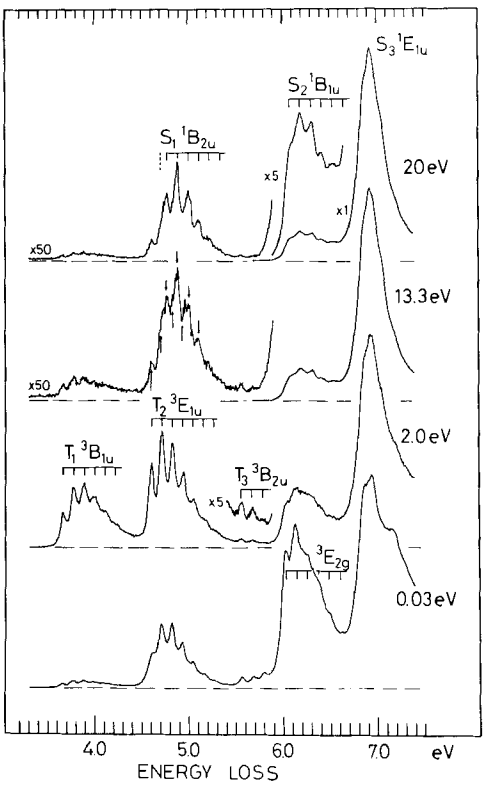

Fig. 5. *Energy-loss spectra in the valence region, obtained with residual energies indicated* (With 20 eV residual energy the spectrum is dominated by the optically allowed transitions, with 0.03 and 2.0 eV by the forbidden singlet-triplet transitions. At intermediate energies both kinds of transitions overlap)

instrument are shown in *Figure 6*. At very low residual energies used here the attenuation of the dipole-allowed $^1B_{1u}$ state is more complete and the structure associated with the forbidden transitions is better visible. The structure is closely spaced and the simplest rationalization appears to be a fit into two progressions with spacings of 0.10 and 0.115 eV and origins at 6.02 and 6.05 eV, indicating in *Figure 6*. The two spacings are consistent with excitation of the ν_2 breathing mode also visible in many other bands. The difference in the origins of the two progressions is less than the frequency of any vibration in benzene and it therefore appears that two different electronic transitions are observed. One of the two transitions is due to the $^3E_{2g}$ valence state. No other valence transition except the $^1E_{2g}$ was predicted in this region by the *ab initio* π-electron calculation of *Hay & Shavitt* [20], and therefore the assignment of the second progression to this $^1E_{2g}$ state seems the most obvious choice, as the sharp peak at 6.33 eV has been reassigned to a *Rydberg* transition in this paper. A much larger singlet-triplet splitting of the two E_{2g} states has been predicted [20], however. A transition involving σ-orbitals, neglected in the π-electron calculation, could also occur in this high-energy region

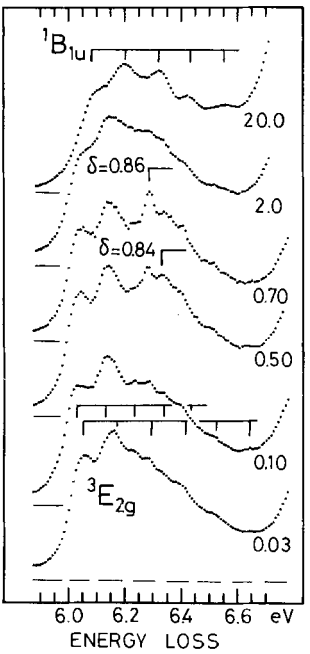

Fig. 6. *Energy-loss spectra in region 4 obtained with residual energies (in eV) indicated* (The true zero of each curve is indicated by a horizontal bar)

and therefore a definitive assignment based on the present data alone does not appear possible. Three more features appear at residual energies of 0.5 and 0.7 eV. They are two narrow peaks at 6.28 and 6.33 eV and a broad underlying hump between 6.2 and 6.5 eV. The two sharp features are assigned to *Rydberg* transitions discussed below. The broad feature was not previously reported and could also correspond to the missing $^1E_{2g}$ transition. Detailed comparison of the present spectra with those of *Wilden & Comer* [4] reveal that they are consistent and the only differences stem from different relative intensities of the features under different scattering conditions. The present spectra with residual energies of 0.03 and 0.1 eV are similar to the residual energy spectrum at 60° and 10 eV of *Wilden & Comer* except that the improved visibility of the $^3E_{2g}$ state in the present study permits the location of the origin one vibrational level lower and the identification of two vibrational progressions. The present spectra with residual energies of 0.5 and 0.7 eV are similar to the 10° to 40°-spectra of *Wilden & Comer*. The 6.33 eV (6.32 eV in [4]) peak is present in both cases but the 6.28 eV peak is visible only under the conditions of the present experiment.

3.2. *Rydberg transitions converging to the first ionization limit.* Optical absorption studies revealed four dipole-allowed *Rydberg* series, one with $\delta = 0.44$ (np) and three with $\delta = 0.08$–0.01 (nf). The latter three series cannot be resolved in the present experiment. These series dominate the spectrum with residual energy of 20 eV in *Figure 7*. Electron impact study revealed a nd-series with $\delta = 0.266$ [4].

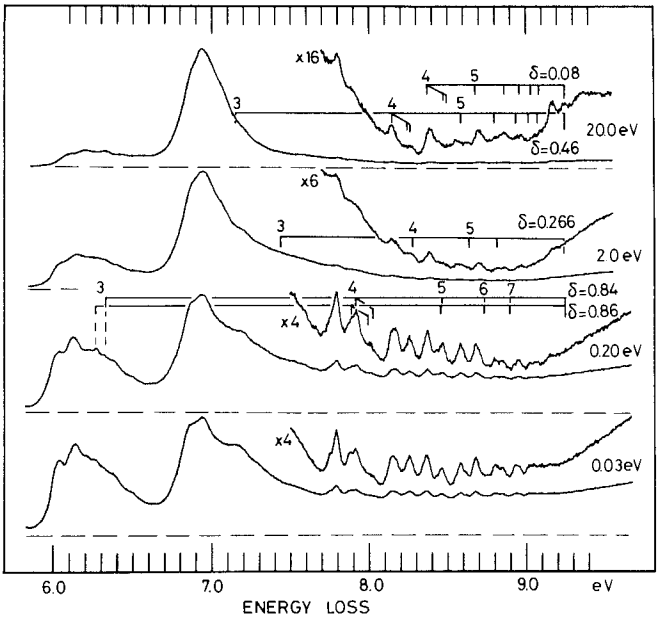

Fig. 7. *Energy-loss spectrum in the Rydberg region* (The residual energy and true zero are given for each curve. Zero has been offset for the vertically expanded curves for clarity. Positions of the two optically allowed series ($\delta = 0.46$ and $\delta = 0.08$), as well as a quadrupole-allowed series ($\delta = 0.266$, [4]) are indicated. The series with $\delta = 0.84$ and $\delta = 0.86$ are the ns-$^1E_{1g}$ [22] and ns-$^3E_{1g}$ (this work) *Rydberg* states)

At the very low residual energies additional peaks at 7.88, 7.92 and 8.45 eV are discernible. These peaks, together with the two peaks at 6.28 and 6.33 eV in region 4 mentioned above can be fitted into the *Rydberg* formula as two series with $\delta = 0.86$ and $\delta = 0.84$. The value of the quantum defect identifies them as ns(a_{1g})-series which has been predicted several times theoretically (*e.g.* [21]). The singlet state $(e_{1g})^3 (a_{1g}3s)^1\ ^1E_{1g}$ has recently been observed in a resonant multiphoton ionization technique at 6.34 eV [22] in a good agreement with the value of 6.33 eV found in this study. The previously unreported peak at 6.28 eV is assigned to the corresponding triplet state $(e_{1g})^3 (a_{1g}3s)^1\ ^3E_{1g}$. In acetylene the singlet-triplet splitting for the two somewhat related states $(\pi_u)^3 (\sigma_g 3s)^1$, $^3\Pi_u$ and $^1\Pi_u$ was found to be 0.09 eV [23]. For the more 'extended' molecule benzene the splitting might plausibly be expected to be somewhat less. The observed splitting of 0.05 eV is in excellent agreement with this expectation. Finally a band has been observed by *Wilden & Comer* [4] at 7.81 eV. *Bolovinos et al.* [5] suggested an assignment to a 4s-band with $\delta = 0.92$. This band also appears in the spectra in *Figure 7*. The corresponding 3s-band would be expected at 6.10 eV. Reference to *Figure 6* shows that the existence of such a band can not be confirmed in this congested region.

Two more forbidden transitions appear as shoulders at 6.86 and 7.15 eV *(Fig. 7)*. Their assignment is difficult because of the large number of π- [20] and possibly σ-transitions expected in this high-energy region and will not be attempted here.

3.3. *Negative ion states.* Good resolution and controlled analyzer transmission down to very low energies has permitted the determination of the excitation functions of individual vibronic levels of the three lowest triplet and the $S_1{}^1E_{1u}$ singlet state for the first time. The excitation functions from about 0.08 to 10 eV above threshold are presented in *Figures 8–10.* Qualitatively they fall into two categories. Excitation of the triplet states have large cross sections at low energies below 12 eV with a number of peaks. In contrast, the cross section for excitation of the $S_3{}^1E_{1u}$ state is relatively low at threshold and increases nearly linearly with residual energy in the first 10 eV range. The cross section recorded at an energy loss of 6.03 eV in the region 4 does not fall into any of these categories and reflects the complex nature of this region with a number of overlapping bands. Information on the electronic excitation in benzene has been obtained previously. *Smyth et al.* [8] measured the total metastable production and luminescence excitation. They observed a number of peaks and interpret them as either resonances or maxima in nonresonant excitation. *Azria & Schulz* [9] measured the excitation of the lowest triplet state from 1 to 10 eV above threshold and ν_1 vibrational excitation from 4 to 10 eV, both at 60°. The triplet excitation in their study was measured at maximum intensity, at an energy loss of 3.9 eV. It is thus most directly comparable to the v=3 excitation curve in *Figure 8* and both curves are consistent in the

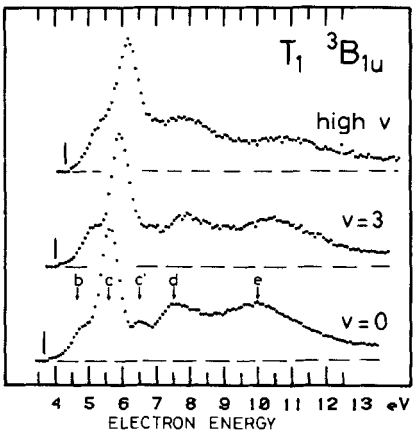

Fig. 8. *Excitation functions of the T_1 state* (The curve marked high v has been obtained at an energy loss of 4.30 eV. Threshold energies are indicated by vertical bars. The resonant states are marked by arrows and labeled according to the classification scheme from [9], with the resonance c′ added)

common energy range. *Azria & Schulz* summarized the information from [8] and [9] and identified seven resonant states which they labeled a–g. The states b–e were found to populate triplet states and their positions, taken from [9], are indicated in *Figures 8–10.* All the features in triplet excitation in *Figures 8–10* correspond to one of the resonant states b–e except that one additional state is discernible in the T_1 v=0 and all T_2 excitation curves. It has been labeled c′ in extension of the classification scheme of *Azria & Schulz* adopted here. The observations from *Figures 8–10* can be summarized as follows:

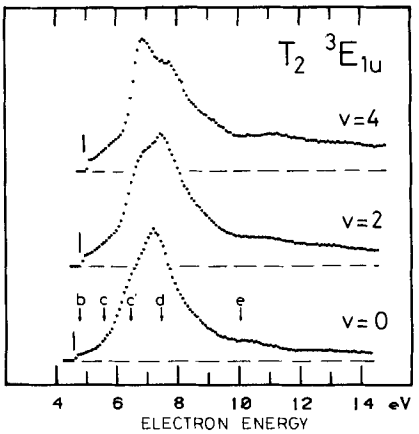

Fig. 9. *Excitation functions of T_2-state, obtained at the vibrational levels given* (The threshold energies and resonances are indicated by vertical bars and arrows)

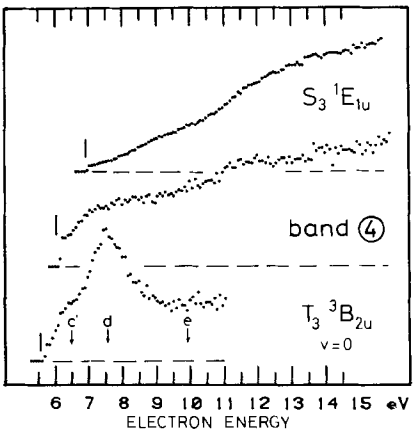

Fig. 10. *Excitation functions of the higher-lying states* (To bypass the background in the excitation function of the T_3 state caused by the tail of the T_2 state, the signal obtained between the v=0 and v=1 levels was subtracted from the T_3 v=0 curve. The curves labeled 'band 4' and S_3 were obtained at energy losses of 6.03 and 6.95 eV, respectively. The excitation functions of the $S_3{}^1E_{1u}$ state contains some contribution from the *Rydberg* state of the same symmetry)

1. The triplet excitation curves consist of a series of broad peaks with widths between approx. 0.5 to 2 eV. Any underlying nonresonant excitation is weaker. The triplet excitation *via* forward electron scattering is resonance-dominated in the first 10 eV above threshold.

2. All five resonant states b, c, c', d, and e populate all the triplet states which are energetically accessible, but not with equal probability, there are prefered decay channels. The $T_1{}^3B_{1u}$ state is populated preferentially by the resonance c, $T_2{}^3E_{1u}$ state by the resonances c' and d, and the $T_3{}^3B_{2u}$ state by the resonance d.

3. The position of a resonance peak depends upon *via* which vibronic level it is observed. It is generally shifted to higher energies with higher vibrational level. Similar effect was observed in the electron impact excitation of the $A^3\Sigma_u^+$ state of N_2 *via* the $A^2\Pi_u$ state of N_2^- [24]. It means that higher parts of the negative-ion potential surface are probed *via* the decay into higher vibrational levels of a given electronic state.

4. There is no resonance to excite the T_1 state near threshold. The cross section is therefore small and this explains why the T_1 state appears with lower intensity in the threshold spectrum in *Figure 5* than *e.g.* the T_2 state which is excited *via* the resonance b at threshold.

In the further discussion the classification of resonances given by *Schulz* [6] will be used. The first kind, a shape resonance, can be pictured as an electron captured in the field of a ground-state molecule. In benzene an electron trapped in the degenerate e_{2u}- and the b_{2g}-orbitals result in the $^2E_{2u}$- and $^2B_{2g}$-shape resonances [7], labeled a and b in [9]. Forming these resonances is a single-electron process and they appear with large intensity in a transmission spectrum ([7] and *Fig. 2*). A second kind are the core-excited shape resonances, pictured as an electron trapped in the field of an excited 'parent' state of a molecule. Forming this kind of a resonance from a ground-state molecule involves a capture of an electron and a simultaneous promotion of 'another' electron, and their formation is less probable. These resonances also appear in the transmission spectrum, albeit with less intensity [25]. On the other hand the core-excited shape resonance will decay into its 'parent' excited state of the neutral molecule with large probability because this process involves solely the escape of one electron. Thus the four peaks c, c', d, and e in *Figures 8–10* are assigned as resulting from decay of core-excited shape resonances in benzene. The low-lying core-excited resonances with the lowest three triplets as parent states will have the configuration $(e_{1g})^3(e_{2u})^2$ which gives rise to states of the $^2B_{1g}$-, $^2B_{2g}$-, $^2E_{1g}$-, and $^4E_{1g}$-symmetries. The doublet states could explain some or all of the peaks c, c', and d. These resonant states will not decay into the three triplet states with equal probability because in some of the decay channels the escape of the electron has to be accompanied by transfer of a remaining electron from one orbital into another and these decay channels will be slower. Thus the present data may provide a key to the assignment of the resonant states if it could be compared with the results of a calculation which predict the approximate energy order and dominant configurations of the core-excited resonances. The first shape resonance, a, is too low in energy to decay into excited electronic states. The second shape resonance, b, with the configuration $(e_{1g})^4(b_{2g})^1$ would not be expected to decay into excited electronic states efficiently because the decay is a two-electron process. The relatively large importance of the resonance b in the excitation of the T_1 and T_2 triplet states observed here is taken as an experimental confirmation of configuration interaction of the resonance b with a core-excited $^2B_{2g}$-resonance.

The role of the intermediate resonant state on the excitation of individual vibrational levels of the two lowest triplets is illustrated in *Figures 11* and *12*. The resolution is constant for all curves and any differences reflect real differences in the envelopes. The shape of the bands is found to depend little on the intermediate

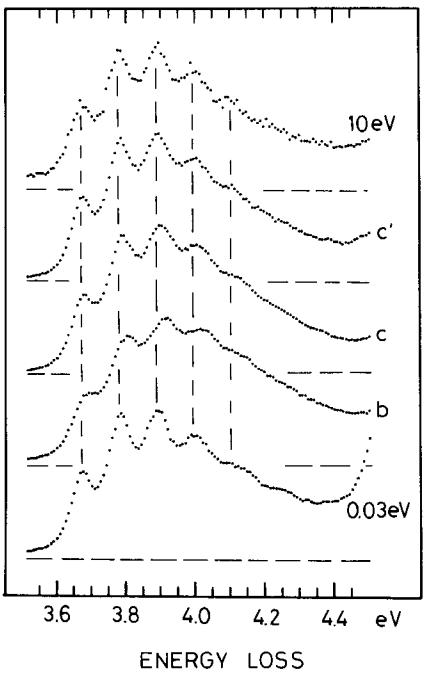

Fig. 11. *The effect of the intermediate resonant state on the T_1-band profile* (The residual energies were chosen such that the excitation proceeded *via* the resonances indicated on the right. The lowest and highest spectra are nonresonant excitation. Note the different profile of the band when excited *via* the resonance b)

resonance except in the case of resonance b where the valleys between the peaks are much less pronounced in both the T_1 and T_2 states and indicate the excitation of additional vibrations. The shape resonance b appears to have a geometry different from the core-excited resonances.

The comparison of the threshold spectrum in *Figure 4* with spectra taken at higher residual energies reveals an effect which at the first sight appears to be an anomalously large intensity of the v=2 vibrational level of the $T_3{}^3B_{2u}$ state. A detailed observation, *Figure 13*, reveals a narrow weak peak constant in incident energy. It appears at an incident energy of 5.87 eV. Based upon this observation a narrow *Feshbach*-type resonance is proposed at this energy, which decays into the quasicontinuum background in the 5.7–5.85 eV energy-loss region with residual energies below 0.15 eV. In this type of resonance two electrons are trapped in a *Rydberg* orbital. They are common in atoms and small molecules [6] but have not yet been observed in molecules of the size of benzene. They usually appear approximately 0.5 eV below their parent *Rydberg* state, thus the $3s(a_{1g})$ *Rydberg* state discussed above suggests itself as the parent state and the *Feshbach* resonance is assigned as the $^2E_{1g}$ state with the dominant configuration $(e_{1g})^3(a_{1g}3s)^2$. A confirmation from a high-sensitivity transmission experiment would be desirable.

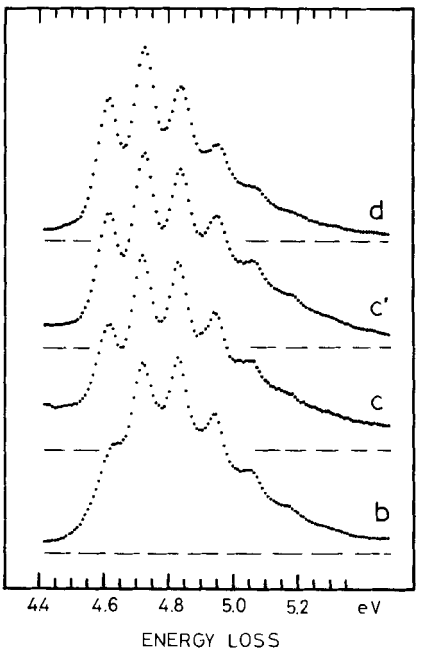

Fig. 12. *The effect of the intermediate resonant state on the T_2-band profile* (The conditions given for *Fig. 11* also apply here. The profile excited *via* the resonance b also differs from the others)

4. Conclusion. – Electron energy loss and excitation spectra of vibronic transitions in benzene were obtained at zero degrees using a new trochoidal electron spectrometer. Even at zero degrees the spectra were found to be dominated by the dipole-forbidden singlet-triplet transitions when very low residual energies less then 2 eV were used. The dipole-forbidden transitions can be identified by their typical excitation functions. The triplet excitation is dominated by core-excited shape resonances. The cross sections are large within a few eV of threshold with several peaks due to the individual resonances and then decrease rapidly. In contrast, the excitation of the dipole-allowed state has only a small cross section at threshold which increases with increasing residual energy. Thus an alternative method to study forbidden transitions emerges using very low residual energies to enhance the forbidden transitions instead of the more conventional variable-angle method. The new instrument has several practical advantages over the classical electrostatical system. Both electron transmission and electron energy loss spectra can be obtained with one instrument. Very low energies down to 0.05 eV can be achieved for both incident and scattered electrons. The new instrument is sensitive, simpler in design and lower in cost. The drawbacks are the limitation to forward scattering and a resolution inferior to the best reported for electrostatic instruments. Thus, whereas the electrostatic instrument will probably remain the ultimate tool for electron scattering, the practical advantages of the new approach make it useful for routine studies of organic compounds.

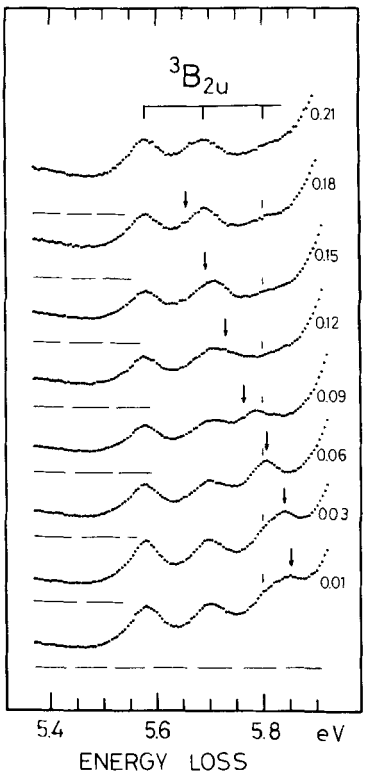

Fig. 13. *Energy-loss spectra in the region 3, recorded with the residual energies (in eV) given* (The positions of the $T_3{}^3B_{2u}$ vibrational levels (vertical bars) and of a weak peak which moves to the left with increasing residual energy (arrows) are indicated. The peak constant in incident energy has been assigned to a $^2E_{1g}$ *Feshbach* resonance in this study)

The very low energy capability coupled with high sensitivity and sufficient resolution enabled the observation of several new features. New *Rydberg* series with $\delta = 0.84$ and $\delta = 0.86$ were observed at very low residual energies and assigned as the ns-$^3E_{1g}$ and $^1E_{1g}$ states.

A new vibrational progression was observed in the complex 6–6.5 eV region. Excitation functions for individual vibronic levels of the three lowest triplets states were obtained, a new peak labeled c′ was found at 6.5 eV and interpreted as a core-excited shape resonance. The preferred decay paths of the resonances were inferred from the spectra. Finally, the existence of a *Feshbach* resonance at 5.87 eV associated with the new *Rydberg* state at 6.28 eV is proposed.

I wish to express my sincere appreciation to Prof. *E. Haselbach* for his continuing support and interest in the present work. I am indebted to *E. Brosi* from the Fribourg machine shop, to *M. Gremaud* from the Fribourg electronic shop, and to the Yale University machine shop for the skillful construction of the apparatus. I thank to *K. D. Jordan* for a helpful discussion and to *W. Chupka* for useful comments on the manuscript. I also thank to my colleagues *T. Bally, P. Suppan, L. Neuhaus, R. Dressler* and *St. Nitsche* for many discussions and general assistance. This work is part of project no. 2.615-0.80 of the *Schweizerischer Nationalfonds zur Förderung der wissenschaftlichen Forschung.*

REFERENCES

[1] *A. Kupperman, W. M. Flicker & O. A. Mosher*, Chem. Rev. *79*, 77 (1979).
[2] *E. N. Lassettre, A. Skerbele, M. A. Dillon & K. J. Ross*, J. Chem. Phys. *48*, 5066 (1968).
[3] *J. P. Doering*, J. Chem. Phys. *51*, 2866 (1969) & *67*, 4065 (1977).
[4] *D. G. Wilden & J. Comer*, J. Phys. B: Atom. Molec. Phys. *13*, 627 (1979).
[5] *A. Bolovinos, J. Philis, E. Pantos, P. Tsekeris & G. Andritsopoulos*, J. Chem. Phys. *75*, 4343 (1981); *J. Philis, A. Bolovinos, G. Andritsopoulos, E. Pantos & P. Tsekeris*, J. Phys. B: At. Mol. Phys. *14*, 3621 (1981).
[6] *G. J. Schulz*, Rev. Mod. Phys. *45*, 378 and 423 (1973).
[7] *K. D. Jordan & P. D. Burrow*, Acc. Chem. Res. *11*, 341 (1978).
[8] *K. C. Smyth, J. A. Schiavone & R. S. Freund*, J. Chem. Phys. *61*, 1782–1788 and 1789 (1974).
[9] *R. Azria & G. J. Schulz*, J. Chem. Phys. *62*, 573 (1975).
[10] *A. Stamatović & G. J. Schulz*, Rev. Sci. Instr. *39*, 1752 (1968) & *41*, 423 (1970).
[11] *D. Spence & O. J. Steingraber*, Argonne National Laboratory Report 1975.
[12] *W. C. Tam & S. F. Wong*, Rev. Sci. Instr. *50*, 302 (1979).
[13] *A. R. Johnston & P. D. Burrow*, J. Elect. Spectr. *25*, 119 (1982).
[14] *G. H. Wannier*, Phys. Rev. *90*, 817 (1953).
[15] *S. Cvejanović & F. H. Read*, J. Phys. B: Atom. Molec. Phys. *7*, 1841 (1974).
[16] *D. Spence*, Phys. Rev. *A 11*, 1539 (1975).
[17] *F. Pichou, A. Huetz, G. Joyez, M. Landau & J. Mazeau*, J. Phys. B: Atom. Molec. Phys. *9*, 933 (1975).
[18] *J. Mazeau, F. Gresteau, R. I. Hall & A. Huetz*, J. Phys. B: Atom. Molec. Phys. *11*, L 557 (1978) and *A. Huetz*, thesis, Paris 1981.
[19] *L. Sanche & M. Michaud*, Chem. Phys. Lett. *80*, 184 (1981).
[20] *P. J. Hay & I. Shavitt*, J. Chem. Phys. *60*, 2865 (1974).
[21] *T. Betts & V. McKoy*, J. Chem. Phys. *54*, 113 (1970).
[22] *K. Krogh-Jespersen, R. P. Rava & L. Goodman*, Chem. Phys. Lett. *64*, 413 (1979); *D. A. Lichtin, R. B. Bernstein & K. R. Newton*, J. Chem. Phys. *75*, 5728 (1981).
[23] *D. G. Wilden, J. Comer & S. Taylor*, J. Phys. B: Atom. Molec. Phys. *13*, 2849 (1980).
[24] *A. Huetz, I. Cadez, F. Gresteau, R. I. Hall, D. Vichon & J. Mazeau*, Phys. Rev. *A 21*, 622 (1980).
[25] *P. Burrow*, private communication.